



Supplement of

**Influence of plant ecophysiology on ozone dry deposition:
comparing between multiplicative and photosynthesis-based
dry deposition schemes and their responses to rising CO₂ level**

Shihan Sun et al.

Correspondence to: Amos P. K. Tai (amostai@cuhk.edu.hk)

The copyright of individual parts of the supplement might differ from the article licence.

Text S1

In this study, we use four long-term measurement sites with hourly observations:

- 25 (1) The Harvard Forest Environmental Measurement Site (referred to as Harvard Forest) located in central Massachusetts. We use a O_3 EC flux dataset together with ambient O_3 concentrations (Munger and Wofsy, 1999) from year 1992 to 2006 to derive v_d . Observed ozone flux data was measured at a height of 29m at the EMS site since 1991 (dataset id: HF004). We use air density at 25°C and 1010hPa to compute v_d when temperature measurements are missing. Observed
30 hourly v_d values are removed if they are: (a) from days with more than 30% of missing hourly measurements are removed; (b) not fall within mean ± 3 standard deviations.
- (2) The Borden Forest Research Station (referred to as Borden Forest) is located in southern Ontario, Canada. We use a database of hourly v_d from year 2008 to 2013 (Wu et al., 2016). G_s was computed using flux data from FLUXNET-Canada Dataset (TEAM, 2016). v_d values were derived with a modified gradient method (MGM) which have been
35 proved to agree well with eddy covariance measurements. Negative v_d values and the same portion of positive v_d values with highest ranking were removed.
- (3) The Blodgett Ameriflux site (referred to as Blodgett Forest) is located near Georgetown, California, US. The site is dominated by ponderosa pine, characterized by a Mediterranean climate. We use the dataset from Fare et al. (2010), which includes observed v_d and G_s from year 2001 to 2007.
- 40 (4) The SMEAR II field measurement station (System for Measuring Forest Ecosystem-Atmosphere Relationships II) is located in Hyytiälä Forest, southern Finland. We use quality-checked hourly O_3 flux and concentrations for Hyytiälä Forest from year 2007 to 2010. The height of trees near measurement tower was about 14-18m from 2000 to 2010. We use O_3 concentrations averaged from measurements at height 33.6m and 16.8m.

45 **Text S2**

The stomatal resistance parameterization for W89 is calculated as described in Wesely (1989) and Wang et al. (1998). The bulk canopy resistance is represented as:

$$R_s = r_s \left\{ 1 + \frac{1}{[200(G+0.1)]^2} \right\} \left\{ \frac{400}{T_s(40-T_s)} \right\} D_i/D_v,$$

where G is solar radiation, T_s is surface air temperature. D_i and D_v are molecular diffusivities for water and the pollutant gas
50 respectively.

The stomatal resistance parameterization for Z03 is calculated as described in Zhang et al. (2003) and Zhang et al. (2002). The expressions to calculate stomatal conductance implemented in TEMIR are also represented here.

$$R_s = 1/[G_s(\text{PAR})f(T)f(\text{VPD})f(\psi)D_i/D_v],$$

55 where $f(T)$, $f(\text{VPD})$ and $f(\psi)$ are dimensionless stress functions for temperature (T), vapor pressure deficit (VPD), and water stress (ψ) respectively as described in Brook et al. (1999). $G_s(\text{PAR})$ is the unstressed canopy stomatal conductance. G_s is calculated as weighted sum of sunlit and shaded leaves.

$$G_s(\text{LAI}, \text{PAR}) = L_{\text{sun}}/r_s(\text{PAR}_{\text{sun}}) + L_{\text{sha}}/r_s(\text{PAR}_{\text{sha}}),$$

$$r_s(\text{PAR}) = r_{\text{smin}}(1 + b_{\text{rs}}/\text{PAR}),$$

60 where L_{sun} and L_{sha} are total sunlit and shaded leaf area index (LAI), PAR_{sun} and PAR_{sha} are absorbed PAR averaged over sunlit and shaded leaves, r_{smin} and b_{rs} are minimum stomatal resistance and empirical light response constant for stomatal resistance. The expression for PAR_{sun} and PAR_{sha} as expressed follows. For $\text{LAI} < 2.5$ or solar radiation $< 200 \text{ Wm}^{-2}$:

$$\text{PAR}_{\text{sha}} = R_{\text{diff}}e^{-0.5\text{LAI}^{0.7}} + 0.07R_{\text{dir}} \times (1.1 - 0.1\text{LAI})e^{-\cos \theta},$$

$$\text{PAR}_{\text{sun}} = \text{PAR}_{\text{sha}} + R_{\text{dir}} \cos \alpha / \cos \theta,$$

65 For the other conditions:

$$\text{PAR}_{\text{sha}} = R_{\text{diff}}e^{-0.5\text{LAI}^{0.8}} + 0.07R_{\text{dir}} \times (1.1 - 0.1\text{LAI})e^{-\cos \theta},$$

$$\text{PAR}_{\text{sun}} = \text{PAR}_{\text{sha}} + R_{\text{dir}}^{0.8} \cos \alpha / \cos \theta,$$

where α is the angle between the leaf and the sun, θ is the solar zenith angle, R_{diff} and R_{dir} are the downward visible radiation fluxes from diffuse and direct-beam radiation above the canopy.

$$70 \quad f(T) = [(T - T_{\text{min}})/(T_{\text{opt}} - T_{\text{min}})] \times [(T_{\text{max}} - T)/(T_{\text{max}} - T_{\text{opt}})]^{bt},$$

$$bt = [(T_{\text{max}} - T_{\text{opt}})/(T_{\text{opt}} - T_{\text{min}})],$$

where T_{min} , T_{max} , T_{opt} are minimum, maximum and optimum temperature respectively.

$$f(D) = 1 - b_{\text{vpd}}D,$$

where b_{vpd} and D are vapour pressure constant and vapour pressure deficit.

$$75 \quad f(\psi) = (\psi - \psi_{c2})/(\psi_{c1} - \psi_{c2}),$$

$$\psi = -0.72 - 0.0013\text{SR},$$

where ψ_{c1} and ψ_{c2} are parameters that specify leaf water potential dependency, SR is solar radiation.

For the photosynthesis-stomatal conductance module in TEMIR, we follow the description by the Community Land Model 4.5 (CLM4.5) (Oleson et al., 2013). A brief summary is also represented here. Photosynthesis in C3 and C4 plants is computed as follows based on Collatz et al. (1992):

$$A_n = \min(A_c, A_j, A_p) - R_d,$$

The Rubisco-limited photosynthetic rate (A_c , $\mu\text{mol m}^{-2}\text{s}^{-1}$) is:

$$A_c = \begin{cases} V_{\text{cmax}} * \frac{c_i - \Gamma^*}{c_i + K_c * (1 + \frac{o_i}{K_o})} & \text{for C3 plants} \\ V_{\text{cmax}} & \text{for C4 plants} \end{cases},$$

85 The RuBP-limited photosynthetic rate (A_j , $\mu\text{mol m}^{-2}\text{s}^{-1}$) is:

$$A_j = \begin{cases} \frac{J}{4} * \frac{c_i - \Gamma^*}{c_i + 2\Gamma^*} & \text{for C3 plants} \\ 2.3 * \varphi & \text{for C4 plants} \end{cases},$$

The product-limited photosynthetic rate (A_p , $\mu\text{mol m}^{-2}\text{s}^{-1}$) is:

$$A_p = \begin{cases} 3 * T_p & \text{for C3 plants} \\ k_p * \frac{c_i}{P_{\text{atm}}} & \text{for C4 plants} \end{cases},$$

The dark respiration (R_d , $\mu\text{mol m}^{-2}\text{s}^{-1}$), which is adjusted by the water stress factor β_t , is given by:

$$90 \quad R_d = \begin{cases} 0.015 * V_{\text{cmax}} * \beta_t & \text{for C3 plants} \\ 0.025 * V_{\text{cmax}} * \beta_t & \text{for C4 plants} \end{cases},$$

In the equations above, c_i is the intercellular CO_2 partial pressure (Pa). K_c and K_o are the Michaelis–Menten constants for carboxylation and oxygenation (Pa). o_i is the intercellular oxygen partial pressure (Pa). Γ^* is the CO_2 compensation point (Pa). V_{cmax} is the maximum rate of carboxylation ($\mu\text{mol m}^{-2}\text{s}^{-1}$). φ is the absorbed PAR ($\mu\text{mol m}^{-2}\text{s}^{-1}$). J is the electron transport rate ($\mu\text{mol m}^{-2}\text{s}^{-1}$). T_p is the triose phosphate utilization rate ($\mu\text{mol m}^{-2}\text{s}^{-1}$), P_{atm} is the ambient atmospheric pressure 95 (Pa), k_p is the initial slope of CO_2 response curve for C4 plants (Pa / Pa). The function β_t ranges from one when soil is wet and to zero when soil is dry.

The stomatal conductance of water g_s ($\mu\text{mol m}^{-2}\text{s}^{-1}$) for FBB and MED is then calculated as in Eq. (4) and Eq. (5) in the main text.

Text S3

We use evaporative-resistance form of Penman-Monteith method to keep consistent with SynFlux stomatal conductance.

The leaf stomatal conductance is:

$$g_w^{-1} = \frac{\varepsilon p (e_s(T_f) - e)}{pE} + (r_a + r_{b,w}),$$

105 where ε is mass ratio between water and dry air, p is air pressure, E is surface moisture flux, T_f is leaf temperature, $e_s(T_f)$ is the saturation vapor pressure at leaf surface. r_a is aerodynamic resistance, $r_{b,w}$ is quasi-laminar layer resistance to water vapor. T_f is estimated as follows:

$$T_f = T + \frac{H(r_a + r_{b,H})}{c_p \rho},$$

110 where T is air temperature, H is sensitive heat, c_p is specific heat of air, ρ is the mass density of air, $r_{b,H}$ is quasi-laminar layer resistance to heat.

Stomatal conductance of O_3 is calculated with molecular diffusion coefficient ratio 0.6 between O_3 and water vapor:

$$g_s = 0.6g_w,$$

115

120

Table S1. References of observational datasets.

Land type group	Lat	Lon	Site	LAI	Canopy Height (m)	Sampling Period	Reference
Deciduous Forest	42.7°N	72.2°W	Harvard Forest	3.4	24	Jan 1991~Dec 1994	Munger et al. (1996)
	42.7°N	72.2°W	Harvard Forest	3.4	24	Jun-Nov, 2000	Wu et al. (2011)
	41.56°N	78.77°W	Kane Experimental Forest, Pennsylvania	1-7	22-23	Apr 29, 1997~Oct 23, 1997	Finkelstein et al. (2000)
	44.3°N	79.9°W	Borden Forest, Ontario, Canada	2.3-4.5	22	01 May, 2008-30 Apr, 2013	Wu et al. (2018)
	44.3°N	80.9°W	Borden Forest, Ontario, Canada	6	18	Aug 2-3, 1988	Padro et al. (1991)
	44.3°N	80.9°W	Borden Forest, Ontario, Canada	0.5	18	Mar 17~Apr 26, 1990	Padro et al. (1992)
	18.3°N	99.7°E	Teak forest in Mea Moh, Thailand	\	12	Jan-Apr 2002	Matsuda et al. (2005)
	18.3°N	99.7°E	Teak forest in Mea Moh, Thailand	\	12	Jan-Aug, 2004	Matsuda et al. (2006)
	51.17°N	0.84°W	Alice Holt, England	\	13	Jul 16 – Aug 18, 2005	Fowler et al. (2009)
	41.7°N	12.35°E	Castelporziano, Italy	3.7	19.7	2012-2013	Fares et al. (2014)
Coniferous Forest	38.9°N	120.6°W	Blodgett Forest, California	3.6	5	Jun 1999~Jun 2000	Kurpius et al. (2002)
	56.3°N	8.4°E	Ulborg Forest, Denmark	8	12	Jun 1994, Sep 1995	Mikkelsen et al. (2000)
	56.3°N	8.4°E	Ulborg Forest, Denmark	8	12	Jan 1996~Dec 2000	Mikkelsen et al. (2004)
	54.8°N	66.9°W	Schefferville, Canada	\	5-6	Jun-Aug 1990	Munger et al. (1996)
	40.0°N	105.5°W	Niwot Ridge AmeriFlux site, Colorado	4.2	11.4	Jun-Aug 2002; May-Sep, 2003; May-Aug, 2005	Turnipseed et al. (2009)
	55.3°N	-3.4°W	Rivox Forest, Scotland	10.2	13	May 23-27, 1992	Coe et al. (1995)
	61.85°N	24.28°E	Hyytiälä, Southern Finland	6	14-18	Aug 2001-Dec 2010	Rannik et al. (2012)
	35.97°N	79.13°W	Blackwood division of Duke forest	3.1	14	Apr 15-May 15 1996	Finkelstein et al. (2000)
	60.4°N	11.1°E	Hurdal, South-East Norway	3.4-4.5	13	Jul 1, 2000-Mar 31, 2003	Hole et al. (2004)
	38.9°N	120.6°W	Blodgett Forest	1.2-2.9	4-7.6	2001-2006	Fares et al. (2010)
Grass	44.2°N	0.7°W	Pine forest in southwestern France	3	15	Jun 9-22, 1992	Lamaud et al. (1994)
	44.2°N	0.7°W	Pine forest in southwestern France	2.1	16~24	Jun 21-Jul 3, 1994; Feb 21-Mar 24, 1997	Lamaud et al. (2002)
Grass	55.79°N	3.24°W	Auchencorth Moss	\	1	Jan 1995~Dec 1998	Fowler et al. (2001)

	40.7°N	8.6°W	Polder Pioito de Sarrazola	2.5-4.5	0.1-0.8	Nov 1994~Oct 1995	Pio et al. (2000)
	37°N	119.8°W	Fresno, California	1	0.2	Jul 8~Aug 6, 1991	Padro et al. (1994)
	10.75°S	62.37°W	Rondonia, Brazil	3.9	\	Jan-Feb, 1999	Sigler et al. (2002)
	45.8°N	8.63°E	Ispra, Italy	\	0.25	Sep 16-23, 1997	Cieslik (2004)
	48.17°N	8.75°E	Klippeneck, Germany	\	0.2	Sep 10-22, 1992	Cieslik (2004)
	40.1°N	88.2°W	Champaign, Illinois	\	0.25-0.3	Jun 26-27, 1982	Droppo et al. (1985)
	34.29°N	85.97°W	Crossville, Alabama	1-2.3	0.1-0.3	Apr 15-Jun 13, 1995	Meyers et al. (1998)
Crop	36.8°N	120.7°W	Fresno, California	1.8-2.7	0.4-0.9	Jul 8~Aug 6, 1991	Padro et al. (1994)
	48.7°N	8°E	Scherzheim, Denmark	\	\	Sep 11-22, 1992	Pilegaard et al. (1998)
	48.85°N	1.97°E	Grignon, France	5.2	2.2	Apr 28, 2008~Sep 9, 2008	Stella et al. (2011)
	44.4°N	0.63°W	La Cape Sud, France	5.1	2.5	Jul 2007~Oct 2007	Stella et al. (2011)
	43.82°N	1.38°E	Lamasquere, France	3.2	2.5	May 2008~Sep 2008	Stella et al. (2011)
	40.05°N	88.37°W	Bondville, Illinois	2.5-3.3	1.8-2.4	Aug 18-Oct 1, 1994	Meyers et al. (1998)
	36.65°N	87.03°W	Nashville, Tennessee	1~6	1.2	Jun 22-Oct 11, 1995	Meyers et al. (1998)
	55.9°N	2.8°W	Gilchriston Farm, Scotland	3	0.3	Jul, 2006	Coyle et al. (2009)
Rainforest	4.97°N	117.85°E	Bukit Atur near Danum Valley	6	30	Apr-Jul, 2008	Fowler et al. (2011)
	10.08°S	61.93°W	Reserva Biologica Juru, Brazil	5.6	40	May 4-22, Sep 21-Oct 20, 1999	Rummel et al. (2007)
	3°S	59.9°W	Reserva Florestal Ducke	7	30	Apr 22-May 8, 1987	Fan et al. (1990)

125 **Table S2. Statistic summary of meteorological variables at long-term sites. Precip: liquid precipitation ($\text{kg m}^{-2} \text{s}^{-1}$); Temp: surface temperature ($^{\circ}\text{C}$); GWR: root zone soil wetness; SWGDN: short wave radiation (W m^{-2}); VPD: vapor pressure deficit (kPa); RH: relative humidity.**

Season	Harvard Forest		Blodgett Forest		Hyttiälä Forest		Borden Forest	
	DJF	JJA	DJF	JJA	DJF	JJA	DJF	JJA
Precip	0.06	0.05	0.07	0.00	0.01	0.01	0.00	0.00
Temp	-2.3	18.6	4.3	19.6	-5.1	15.3	-4.4	19.9
GWR	0.58	0.38	0.42	0.26	0.62	0.60	0.669	0.50
SWGDN	72	225	97	343	11	191	64	273
RH	0.82	0.84	0.66	0.42	0.91	0.74	0.92	0.75
VPD	0.09	0.38	0.29	1.39	0.04	0.49	0.04	0.67

130

Table S3. PFT and land category mapping among CLM, Z03 and W89.

CLM PFT	Z03 surface type	W89 surface type
Needleleaf evergreen tree - temperate	Evergreen needleleaf trees	Coniferous forest
Needleleaf evergreen tree - boreal		
Needleleaf deciduous tree - boreal	Deciduous needleleaf trees	
Broadleaf evergreen tree - tropical	Tropical broadleaf trees	Amazon forest
Broadleaf deciduous tree - tropical	Deciduous broadleaf trees	Deciduous forest
Broadleaf deciduous tree - temperate		
Broadleaf deciduous tree - boreal		
Broadleaf evergreen shrub - temperate	Thorn shrubs	Shrub/grassland
Broadleaf deciduous shrub - temperate	Deciduous shrubs	
Broadleaf deciduous shrub - boreal		
C₃ arctic grass	Tundra	Tundra
C₃ non-arctic grass	Short grass	Shrub/grassland
C₄ grass	Corn	
C₃ crop	Crops	Agricultural land
C₃ irrigated		

Table S4. List of abbreviations used in this paper with descriptions.

Symbol	Description
A_n	leaf net CO ₂ assimilation rate
BVOC	biogenic volatile organic compounds
CLM	Community Land Model
CRO	Crop
C_s	CO ₂ concentration at the leaf surface
CTMs	chemical transport models
DBF	Deciduous Broadleaf Forest
D_i	molecular diffusivities for water
DO₃SE	The Deposition of O ₃ for Stomatal Exchange
D_v	molecular diffusivities for pollutant gas
ENF	Evergreen Needleleaf Forest
ESMs	Earth system models
FBB	Farquhar-Ball-Berry stomatal scheme
g^0	PFT-dependent minimum stomatal conductance
g_{1B}	fitted slope parameter for Ball-Berry model
g_{1M}	fitted slope parameter for Medlyn model
GRA	Grass
G_c	Canopy conductance
G_s	Canopy stomatal conductance
h_s	leaf surface relative humidity
L	Obukhov length
LAI	leaf area index
L^{sha}	shaded LAI
LSMs	land surface models
L^{sun}	sunlit LAI
MAP	mean annual precipitation
MED	Medlyn stomatal scheme
MERRA-2	Modern-Era Reanalysis for Research and Applications version 2
MODIS	Moderate Resolution Imaging Spectroradiometer
NMAEF	normalized mean absolute error factor
NMBF	normalized mean bias factor
NO	nitric oxide
O₃	ozone

P-M	Penman-Monteith
PAR	photosynthetically active radiation
PFTs	plant functional types
P_r	the Prandtl number for air
R^2	R -squared value
R_a	aerodynamic resistance
R_{ac}	in-canopy aerodynamic resistance
R_{adc}	lower canopy aerodynamic resistance
R_{ag}	ground aerodynamic resistance
R_b	quasi-laminar sublayer resistance
r_b	leaf boundary resistance
R_c	bulk surface resistance
R_c	canopy resistance
R_{clx}	lower canopy resistance
R_{cut}	cuticular resistance
R_{cutd0}	reference cuticular resistance for dry condition
R_{cutw0}	reference cuticular resistance for wet condition
R_g	ground resistance
RH	relative humidity
R_s	stomatal resistance
r_{smin}	minimum stomatal resistance
r_s^{sha}	shaded stomatal resistance
r_s^{sun}	sunlit stomatal resistance
RuBP	ribulose 1,5-bisphosphate
S_r	the Schmidt number
SRAD	incoming shortwave solar radiation
SW	soil wetness
T	surface temperature
TEMIR	Terrestrial Ecosystem Model in R
TRF	Tropical Rainforest
u^*	friction velocity
v_d	dry deposition velocity of O ₃
VPD	vapor pressure deficit
W89	Wesely deposition scheme
W89FBB	Wesely deposition scheme replaced with Faquhar-Ball-Berry stomatal scheme

W89MED	Wesely deposition scheme replaced with Medlyn stomatal scheme
W_{st}	stomatal blocking factor
z	reference height
z_0	roughness height
Z03	Zhang et al. (2003) deposition scheme
Z03FBB	Zhang et al. (2003) deposition scheme replaced with Faquhar-Ball-Berry stomatal scheme
Z03MED	Zhang et al. (2003) deposition scheme replaced with Medlyn stomatal scheme
κ	von Kármán constant
ψ	water stress

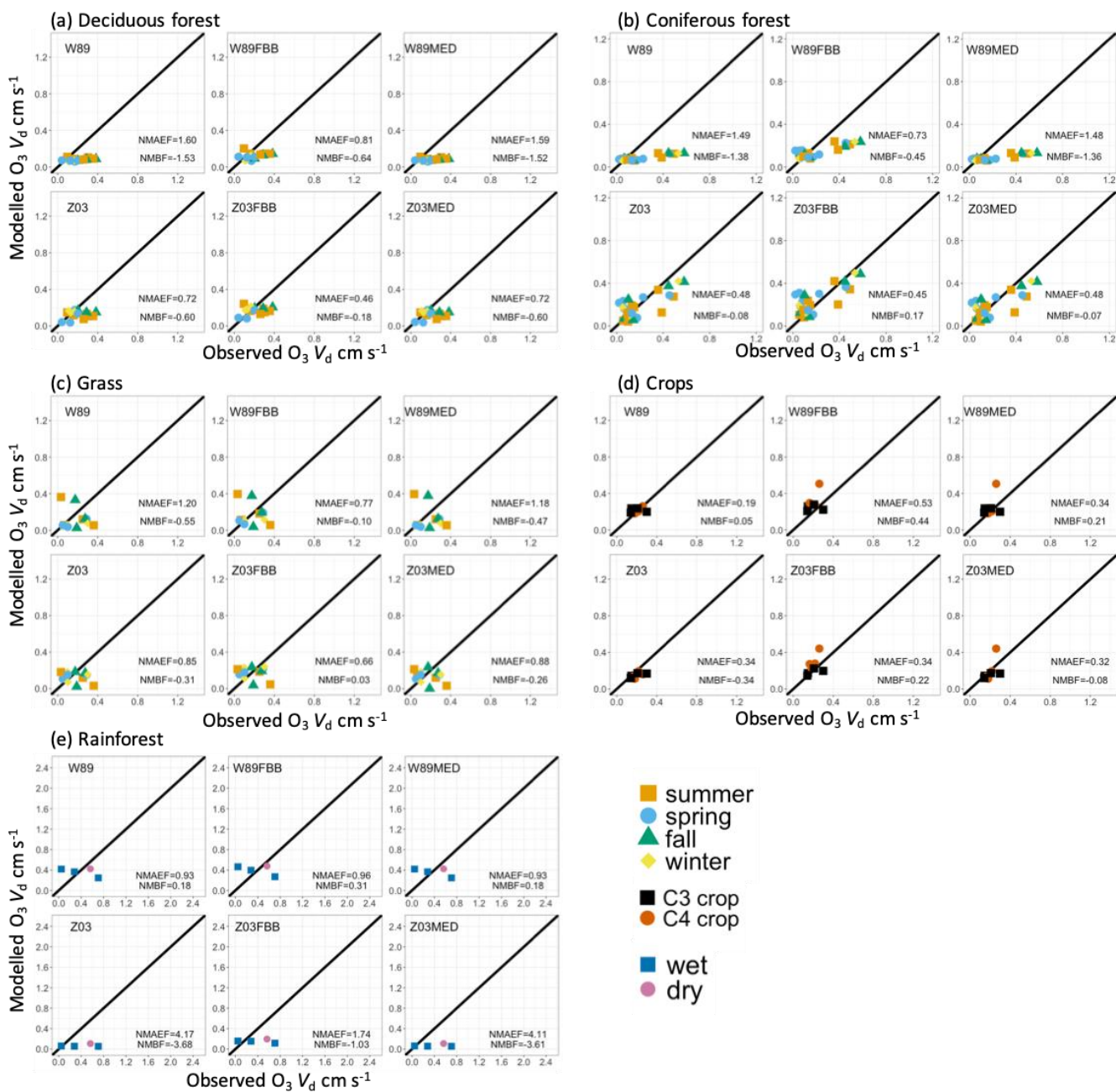


Figure S1. Average nighttime (LT 22:00pm~4:00am) observed-simulated dry deposition velocities for five land types. Colours indicate dominant seasons during field measurements, except that for crops different colours indicate crop types (C3 and C4 crops).

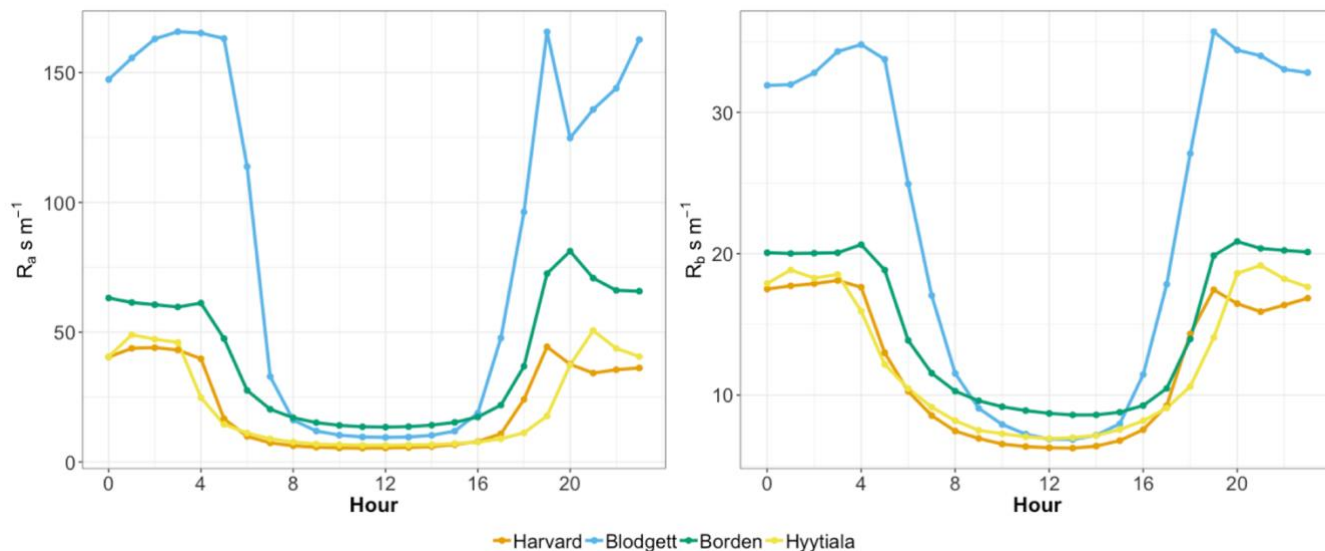


Figure S2. Average JJA diurnal aerodynamic resistance (R_a) and boundary layer resistance (R_b) at long-term measurement sites.

150 References in the Supplementary

- Cieslik, S. A.: Ozone uptake by various surface types: a comparison between dose and exposure, *Atmos. Environ.*, 38, 2409-2420, <https://doi.org/10.1016/j.atmosenv.2003.10.063>, 2004.
- Coe, H., Gallagher, M. W., Choularton, T. W., and Dore, C.: Canopy Scale Measurements of Stomatal and Cuticular O₃ Uptake by Sitka Spruce, *Atmos. Environ.*, 29, 1413-1423, [https://doi.org/10.1016/1352-2310\(95\)00034-V](https://doi.org/10.1016/1352-2310(95)00034-V), 1995.
- Collatz, G. J., Ribas-Carbo, M., and Berry, J. A.: Coupled Photosynthesis-Stomatal Conductance Model for Leaves of C4 Plants, *Aust. J. Plant Physiol.*, 19, 519-538, <https://doi.org/10.1071/Pp9920519>, 1992.
- 160 Coyle, M., Nemitz, E., Storeton-West, R., Fowler, D., and Cape, J. N.: Measurements of ozone deposition to a potato canopy, *Agr. Forest Meteorol.*, 149, 655-666, <https://doi.org/10.1016/j.agrformet.2008.10.020>, 2009.
- Fan, S. M., Wofsy, S. C., Bakwin, P. S., Jacob, D. J., and Fitzjarrald, D. R.: Atmosphere-Biosphere Exchange of CO₂ and O₃ in the Central Amazon Forest, *J. Geophys. Res.-Atmos.*, 95, 16851-16864, <https://doi.org/10.1029/JD095iD10p16851>, 1990.
- 165 Finkelstein, P. L., Ellestad, T. G., Clarke, J. F., Meyers, T. P., Schwede, D. B., Hebert, E. O., and Neal, J. A.: Ozone and sulfur dioxide dry deposition to forests: Observations and model evaluation, *J. Geophys. Res.-Atmos.*, 105, 15365-15377, <https://doi.org/10.1029/2000jd900185>, 2000.
- 170 Fowler, D., Flechard, C., Cape, J. N., Storeton-West, R. L., and Coyle, M.: Measurements of ozone deposition to vegetation quantifying the flux, the stomatal and non-stomatal components, *Water Air Soil Poll.*, 130, 63-74, <https://doi.org/10.1023/A:1012243317471>, 2001.

- 175 Fowler, D., Nemitz, E., Miszta, P., Di Marco, C., Skiba, U., Ryder, J., Helfter, C., Cape, J. N., Owen, S., Dorsey, J., Gallagher, M. W., Coyle, M., Phillips, G., Davison, B., Langford, B., MacKenzie, R., Muller, J., Siong, J., Dari-Salisburgo, C., Di Carlo, P., Aruffo, E., Giammaria, F., Pyle, J. A., and Hewitt, C. N.: Effects of land use on surface-atmosphere exchanges of trace gases and energy in Borneo: comparing fluxes over oil palm plantations and a rainforest, *Philos. T. R. Soc. B.*, 366, 3196-3209, <https://doi.org/10.1098/rstb.2011.0055>, 2011.
- 180 Kurpius, M. R., McKay, M., and Goldstein, A. H.: Annual ozone deposition to a Sierra Nevada ponderosa pine plantation, *Atmos. Environ.*, 36, 4503-4515, [https://doi.org/10.1016/S1352-2310\(02\)00423-5](https://doi.org/10.1016/S1352-2310(02)00423-5), 2002.
- 185 Lamaud, E., Brunet, Y., Labatut, A., Lopez, A., Fontan, J., Druilhet, A.: The Landes experiment: biosphere-atmosphere exchanges of ozone and aerosol particles above a pine forest. *J. Geophys. Res.*, 99, 16511-16521, <https://doi.org/10.1029/94JD00668>, 1994.
- Lamaud, E., Carrara, A., Brunet, Y., López, A., & Druilhet, A.: Ozone fluxes above and within a pine forest canopy in dry and wet conditions. *Atmos. Environ.*, 36, 77-88, [https://doi.org/10.1016/S1352-2310\(01\)00468-X](https://doi.org/10.1016/S1352-2310(01)00468-X), 2002.
- 190 Meyers, T. P., Finkelstein, P., Clarke, J., Ellestad, T. G., and Sims, P. F.: A multilayer model for inferring dry deposition using standard meteorological measurements, *J. Geophys. Res.-Atmos.*, 103, 22645-22661, <https://doi.org/10.1029/98jd01564>, 1998.
- 195 Mikkelsen, T. N., Ro-Poulsen, H., Pilegaard, K., Hovmand, M. F., Jensen, N. O., Christensen, C. S., and Hummelshøj, P.: Ozone uptake by an evergreen forest canopy: temporal variation and possible mechanisms, *Environ. Pollut.*, 109, 423-429, [https://doi.org/10.1016/S0269-7491\(00\)00045-2](https://doi.org/10.1016/S0269-7491(00)00045-2), 2000.
- 200 Munger, J. W., Wofsy, S. C., Bakwin, P. S., Fan, S. M., Goulden, M. L., Daube, B. C., Goldstein, A. H., Moore, K. E., and Fitzjarrald, D. R.: Atmospheric deposition of reactive nitrogen oxides and ozone in a temperate deciduous forest and a subarctic woodland .1. Measurements and mechanisms, *J. Geophys. Res.-Atmos.*, 101, 12639-12657, <https://doi.org/10.1029/96jd00230>, 1996.
- 205 Munger, W., and Wofsy, S.: Canopy-atmosphere exchange of carbon, water and energy at Harvard Forest EMS Tower since 1991, Harvard Forest Data Archive: HF004, 1999.
- Oleson, K., Lawrence, D., Bonan, G., Drewniak, B., Huang, M., Koven, C., Levis, S., Li, F., Riley, W., and Subin, Z.: Technical description of version 4.5 of the Community Land Model (CLM), NCAR Technical Note: NCAR/TN-503+ STR, National Center for Atmospheric Research (NCAR), Boulder, CO, USA, <https://doi.org/10.5065/D6RR1W7M>, 2013.
- 210 Padro, J., Massman, W. J., Shaw, R. H., Delany, A., and Oncley, S. P.: A Comparison of Some Aerodynamic Resistance Methods Using Measurements over Cotton and Grass from the 1991 California Ozone Deposition Experiment, *Bound.-Lay. Meteorol.*, 71, 327-339, <https://doi.org/10.1007/Bf00712174>, 1994.
- 215 Pilegaard, K., Hummelshøj, P., and Jensen, N. O.: Fluxes of ozone and nitrogen dioxide measured by eddy correlation over a harvested wheat field, *Atmos. Environ.*, 32, 1167-1177, [https://doi.org/10.1016/S1352-2310\(97\)00194-5](https://doi.org/10.1016/S1352-2310(97)00194-5), 1998.
- Pio, C. A., Feliciano, M. S., Vermeulen, A. T., and Sousa, E. C.: Seasonal variability of ozone dry deposition under southern European climate conditions, in Portugal, *Atmos. Environ.*, 34, 195-205, [https://doi.org/10.1016/S1352-2310\(99\)00276-9](https://doi.org/10.1016/S1352-2310(99)00276-9), 2000.
- 220 Rannik, U., Altimir, N., Mammarella, I., Back, J., Rinne, J., Ruuskanen, T. M., Hari, P., Vesala, T., and Kulmala, M.: Ozone deposition into a boreal forest over a decade of observations: evaluating deposition partitioning and driving variables, *Atmos. Chem. Phys.*, 12, 12165-12182, <https://doi.org/10.5194/acp-12-12165-2012>, 2012.

- 225 Rummel, U., Ammann, C., Kirkman, G. A., Moura, M. A. L., Foken, T., Andreae, M. O., and Meixner, F. X.: Seasonal variation of ozone deposition to a tropical rain forest in southwest Amazonia, *Atmos. Chem. Phys.*, 7, 5415-5435, <https://doi.org/10.5194/acp-7-5415-2007>, 2007.
- 230 Sigler, J. M., Fuentes, J. D., Heitz, R. C., Garstang, M., and Fisch, G.: Ozone dynamics and deposition processes at a deforested site in the Amazon Basin, *Ambio.*, 31, 21-27, <https://doi.org/10.1579/0044-7447-31.1.21>, 2002.
- Stella, P., Personne, E., Loubet, B., Lamaud, E., Ceschia, E., Beziat, P., Bonnefond, J. M., Irvine, M., Keravec, P., Mascher, N., and Cellier, P.: Predicting and partitioning ozone fluxes to maize crops from sowing to harvest: the Surf atm-O₃ model, *Biogeosciences*, 8, 2869-2886, <https://doi.org/10.5194/bg-8-2869-2011>, 2011.
- 235 TEAM, F. C.: FLUXNET Canada Research Network-Canadian Carbon Program Data Collection, 1993-2014, ORNL DAAC, 2016.
- 240 Turnipseed, A. A., Burns, S. P., Moore, D. J. P., Hu, J., Guenther, A. B., and Monson, R. K.: Controls over ozone deposition to a high elevation subalpine forest, *Agr. Forest Meteorol.*, 149, 1447-1459, <https://doi.org/10.1016/j.agrformet.2009.04.001>, 2009.
- Wu, Z. Y., Wang, X. M., Chen, F., Turnipseed, A. A., Guenther, A. B., Niyogi, D., Charusombat, U., Xia, B. C., Munger, J. W., and Alapaty, K.: Evaluating the calculated dry deposition velocities of reactive nitrogen oxides and ozone from two community models over a temperate deciduous forest, *Atmos. Environ.*, 45, 2663-2674, <https://doi.org/10.1016/j.atmosenv.2011.02.063>, 2011.
- 245 Wu, Z. Y., Staebler, R., Vet, R., and Zhang, L. M.: Dry deposition of O₃ and SO₂ estimated from gradient measurements above a temperate mixed forest, *Environ. Pollut.*, 210, 202-210, <https://doi.org/10.1016/j.envpol.2015.11.052>, 2016.
- 250 Wu, Z. Y., Schwede, D. B., Vet, R., Walker, J. T., Shaw, M., Staebler, R., and Zhang, L. M.: Evaluation and Intercomparison of Five North American Dry Deposition Algorithms at a Mixed Forest Site, *J. Adv. Model Earth Sy.*, 10, 1571-1586, <https://doi.org/10.1029/2017ms001231>, 2018.
- 255 Zhang, L. M., Moran, M. D., Makar, P. A., Brook, J. R., and Gong, S. L.: Modelling gaseous dry deposition in AURAMS: a unified regional air-quality modelling system, *Atmos. Environ.*, 36, 537-560, [https://doi.org/10.1016/S1352-2310\(01\)00447-2](https://doi.org/10.1016/S1352-2310(01)00447-2), 2002.
- 260 Zhang, L., Brook, J. R., and Vet, R.: A revised parameterization for gaseous dry deposition in air-quality models, *Atmos. Chem. Phys.*, 3, 2067-2082, <https://doi.org/10.5194/acp-3-2067-2003>, 2003.